Mathematical Biosciences and Engineering

MBE, 20 (6): 10358–10375.
DOI: 10.3934/mbe.2023454
Received: 10 January 2023
Revised: 19 March 2023
Accepted: 20 March 2023
Published: 03 April 2023

http://www.aimspress.com/journal/MBE

Research article

Indoor high-precision visible light positioning system using Jaya algorithm

Cuicui Cai[1], Maosheng Fu[1], Xianmeng Meng[2], Chaochuan Jia[1,*] and Mingjing Pei[1]

[1] School of Electronics and Information Engineering, West Anhui University, Lu'an 237012, China
[2] School of Computer Science and Information Engineering, Hefei University of Technology, Hefei 230601, China

* **Correspondence:** Email: ccjia@hfcas.ac.cn.

Abstract: Several indoor positioning systems that utilize visible light communication (VLC) have recently been developed. Due to the simple implementation and high precision, most of these systems are dependent on received signal strength (RSS). The position of the receiver can be estimated according to the positioning principle of the RSS. To improve positioning precision, an indoor three-dimensional (3D) visible light positioning (VLP) system with the Jaya algorithm is proposed. In contrast to other positioning algorithms, the Jaya algorithm has a simple structure with only one phase and achieves high accuracy without controlling the parameter settings. The simulation results show that an average error of 1.06 cm is achieved using the Jaya algorithm in 3D indoor positioning. The average errors of 3D positioning using the Harris Hawks optimization algorithm (HHO), ant colony algorithm with an area-based optimization model (ACO-ABOM), and modified artificial fish swam algorithm (MAFSA) are 2.21 cm, 1.86 cm and 1.56 cm, respectively. Furthermore, simulation experiments are performed in motion scenes, where a high-precision positioning error of 0.84 cm is achieved. The proposed algorithm is an efficient method for indoor localization and outperforms other indoor positioning algorithms.

Keywords: indoor positioning system; received signal strength; visible light communication; Jaya algorithm; location accuracy

1. Introduction

With the rapid development of wireless communication, the demand for location-based services (LBS) exhibited a significant growth trend [1,2]. In the positioning field, global positioning systems (GPSs) are extensively applied to outdoor positioning for high location precision and low cost. When a GPS is applied in the indoor environment, it has low accuracy owing to the severe attenuation of satellite signal strength [3]. To meet the increasing need for indoor positioning services, positioning systems with Bluetooth [4], wireless local area networks [5], and ultra-wide-band radio [6] technologies are used. These positioning systems are limited due to several factors, such as low accuracy, additional infrastructure, narrow tracking range, and low scalability. However, new indoor positioning systems with VLC have been proposed. VLC-based systems have the advantages of high precision, low cost, less additional equipment, and good security [7,8].

According to different receivers, indoor VLP systems could be classified into two types: image sensor-based (IS-based) [9] and photodiode-based (PD-based) [10]. The IS-based VLP systems require only a CMOS camera and use image processing technology to achieve highly accurate positioning. Guan et al. [11] presented a high-accuracy indoor robot VLP system, and the proposed system had a positioning accuracy within 1 cm and an average computational time of 0.08 s. Chen et al. [12] proposed a simultaneous localization and calibration VLP method based on double coplanar circular LED lights, and the proposed system on mobile devices obtained a mean positioning accuracy of 7.91 cm and an average delay time of 0.182 s.

The PD-based VLP systems employ several positioning algorithms to estimate the position of the PD, including RSS, angle of arrival (AOA), time difference of arrival (TDOA), and time of arrival (TOA) [13–15]. Due to the limited distances between the transmitters and the receivers and the high optical transmission rates, small-time errors can lead to large position estimation errors. Hence, TOA and TDOA technologies require the use of strictly synchronized clock cycles for all transmitters, which increases the complexity of the VLP system. Because of the camera's limited field of view (FOV), AOA technology requires a very dense lighting grid, and this also increases the complexity and cost of the VLP system. In contrast, the indoor RSS-based VLP system easily estimates the location according to the RSS, resulting in a high-precision positioning. Consequently, several RSS-based VLP systems have been proposed [10,16,17].

The well-known intelligent optimization algorithms are efficient for solving nonlinear optimization problems. Several complex problems have been solved using intelligent algorithms [18–23]. However, the problem of indoor 3D positioning can be seen as a global optimization problem. Many researchers have presented several indoor VLP systems with intelligent optimization algorithms. Chen et al. [24] improved the genetic algorithm (GA) and used it for an indoor localization system. The results obtained using this algorithm show that it could effectively reduce location errors. Chen et al. [25] presented a hybrid bat algorithm and applied it to an indoor positioning system. The average location error of the positioning system was 1.16 cm. Li et al. [26] proposed a VLP method using the bat algorithm and achieved fast localization, but the positioning accuracy of the algorithm could be improved. Chen et al. [27] analyzed the effect of environmental interference and presented a modified particle swarm optimization algorithm, which was applied to an indoor VLP system. The location system obtained an average location error of 3.12 cm. Wu et al. [28] applied a differential evolution algorithm to an indoor VLP system. This system provided high-speed positioning with a location error as low as 0.69 cm. The aforementioned optimization algorithms in the PD-based VLP system could achieve high-

accuracy, however, the algorithms require the execution of multiple phases and have a high level of complexity.

Some RSS-based VLP systems that use artificial neural networks (ANNs) and intelligent algorithms have been presented in recent years. Guan et al. [29] utilized a modified GA and ANN for an indoor positioning system, and a location error of 1.02 cm was obtained. Mahmoud et al. [30] developed a multilayer perceptron neural network and used it for an indoor VLP system, which accurately estimated the location with an average error of 1.98 cm. This type of VLP system has a high positioning accuracy. However, it requires the use of data to train the network, which may require additional computational time.

To solve these problems, an indoor high-precision VLP system based on the Jaya algorithm is presented. As a novel intelligent optimization algorithm, the Jaya algorithm performs using only common control parameters [31]. Due to the simple structure of the Jaya algorithm with only one stage, it is calculated in a short computational time and can be simply implemented for indoor positioning. The main contributions of this paper are as follows.

1) The indoor visible positioning system model is described, the problem of position optimization estimation is explained, and the Jaya algorithm is used to address the problem.

2) The positioning performance of the Jaya algorithm is validated with multipoint tests in stationary and motion scenes, and the positioning accuracy of the indoor VLP system has been effectively improved.

This paper can be organized as follows. The indoor 3D positioning system model and the VLC channel model are presented in Section 2. The Jaya algorithm for 3D positioning is described in Section 3. Section 4 describes the experimental simulations and analysis. Finally, Section 5 depicts the conclusions and future work.

2. System model

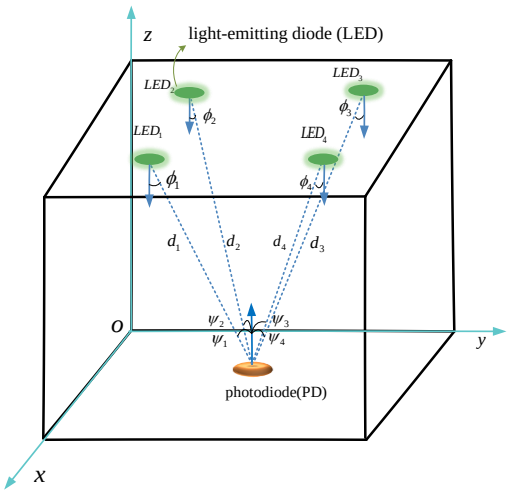

Figure 1. Typical indoor VLP system model.

The model of the VLP system for a typical indoor environment is illustrated in Figure 1. The system mainly consists of light-emitting diodes (LEDs) and a PD. Four LEDs are mounted on the ceiling of the room as signal generators and illumination source. Each LED has a unique ID

information that is closely related to the 3D coordinates, and the ID information is transmitted after modulation using the code division multiple access (CDMA) scheme [24]. As a receiver, the PD can receive signals from different LEDs and obtain ID information by demodulation. According to the RSS method, the distance between the receiver and the transmitter is calculated from the signal strength received, and the position of the PD is estimated [32].

The signal transmission path of the transmitter consists mainly of the line-of-sight (LOS) path and non-line-of-sight (NLOS) path in a VLC system [33,34]. The channel model of the VLC system is presented in Figure 2. It is deduced from [35] that the received power of the LOS path accounts for more than 95% of the total received power. Therefore, the influence of the directed light mainly determines the performance of the VLC system, and this study only considered the LOS path of the signal transmission.

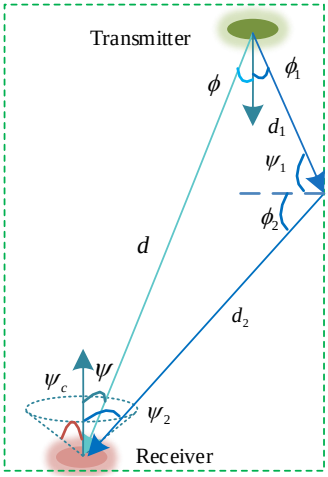

Figure 2. Channel model of the VLC system.

Due to the long distance transmission of light and the large beam divergence of the LEDs, the LEDs can be seen as Lambert radiation, and the direct current gain of the channel is calculated as [36]

$$H(0)_{LOS} = \begin{cases} \dfrac{(m+1)A}{2\pi d^2}\cos^m(\phi)T_s(\psi)g(\psi)\cos(\psi), & 0 \le \psi \le \psi_c \\ 0, & \psi > \psi_c \end{cases}, \tag{1}$$

where A denotes the PD's effective area, ϕ denotes the angle of irradiance, ψ represents the angle of incidence, ψ_c represents the FOV of the receiver, $T_s(\psi)$ and $g(\psi)$ respectively represent the gain of the optical filter and the optical concentrator, d denotes the distance between the LED and PD, and m represents the Lambert parameter expressed as

$$m = -\log 2 / \log(\cos(\phi_{1/2})), \tag{2}$$

where $\phi_{1/2}$ is the half-power angle of the LED.

Then, $g(\psi)$ can be computed as

$$g(\psi)=\begin{cases}\dfrac{n^2}{\sin^2(\psi_c)}, & 0\le\psi\le\psi_c\\ 0, & \psi>\psi_c\end{cases}, \tag{3}$$

where n is the PD's refractive index.

Assuming that the transmitting signal power of the LED is defined as P_t, and the receiving signal power of PD is given by

$$P_r = P_t \times H(0)_{LOS}. \tag{4}$$

The total noise variance of the location system σ^2_{noise} is composed of the thermal noise variance $\sigma^2_{thermal}$, shot noise variance σ^2_{shot}, and inter-symbol interference P_{risi}. The total noise of the system is typically represented by an additive white Gaussian noise (AWGN) model [10]. The RSS of the PD is determined by the value of the signal-to-noise ratio (SNR), represented as [27]:

$$SNR = 10\log_{10}\frac{(P_r R_p)^2}{\sigma^2_{shot}+\sigma^2_{thermal}+(P_{risi})^2}, \tag{5}$$

where R_p represents the transformation efficiency.

3. Jaya algorithm for 3D positioning

According to the aforementioned system model, the high-precision indoor location problem is to search for the optimal position in an interior space. The Jaya algorithm as one of the intelligent optimization algorithms can be used for indoor positioning [37]. It has a simple structure with only one stage and is used in a variety of applications [31,38]. The specific stage of the Jaya algorithm can be expressed as Eq (6) [37].

$$x_{newi,j} = x_{i,j} + r_1\cdot(x_{best,j}-|x_{i,j}|) - r_2\cdot(x_{worst,j}-|x_{i,j}|), \tag{6}$$

where $x_{newi,j}$ represents the new solution of $x_{i,j}$, $x_{i,j}$ denotes the *j*-th variable of the *i*-th candidate solution, $x_{best,j}$ and $x_{worst,j}$ are respectively the *j*-th variable of the best solution and the worst solution, $|x_{i,j}|$ represents the absolute value of $x_{i,j}$, and r_1 and r_2 are random numbers that obey a normal distribution in the range [0,1]. The detail of the Jaya algorithm is presented in Figure 3.

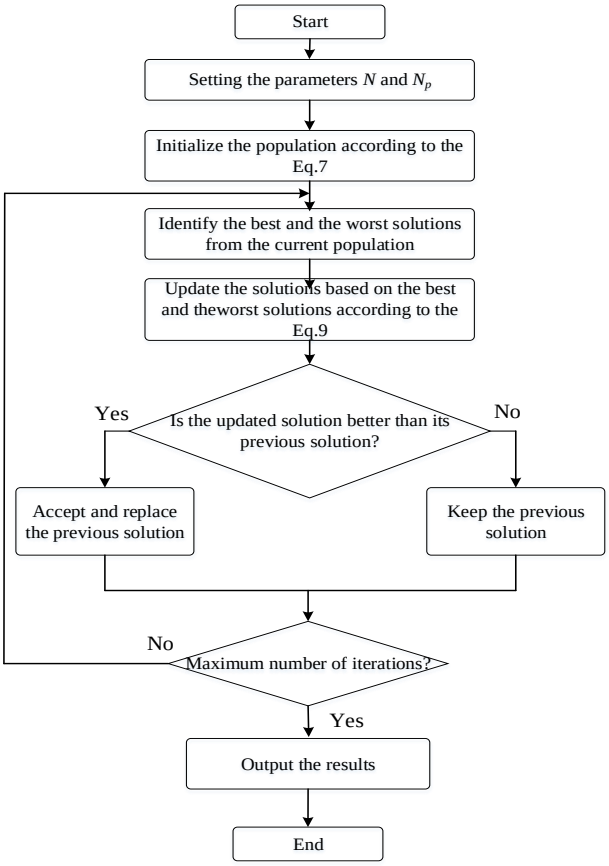

Figure 3. Flowchart of the proposed algorithm.

The detailed optimization procedure for indoor 3D positioning is described as follows:

Step 1: Setting the parameters.

The main parameters need to be set before the algorithm is executed. These parameters consist of the population size N_p, variable dimension D, maximum number of iterations N, and search space $[Lb_j, Ub_j]$.

Step 2: Initialize the algorithm.

A random position is given to each individual as PD's initiation position. The location is limited by room size. The initial population $X_{i,0}$ can be represented as

$$X_{i,0}=Lb_i + rand \times (Ub_i - Lb_i),\ i = 1, 2, ...N_p. \tag{7}$$

Step 3: Calculate the value of the fitness function of each individual.

According to the indoor positioning system model, the fitness function is given by [39].

$$Fitness(x, y, z) = \sum_{i=1}^{4} (P_r^i - \hat{P}_r^i)^2, \tag{8}$$

where P_r^i represents the RSS of the test point for the *i*-th LED, and $\hat{P}_r^i$ denotes the RSS of the estimated point for the *i*-th LED.

Through the calculation of the individual fitness function values, the positions that have the worst and best values are then selected.

Step 4: Generating a new population.

In this step, a new position is generated, denoted as

$$X_{i,G+1} = X_{i,G} + r_1 \times (X_{i,best} - |X_{i,G}|) - r_2 \times (X_{i,worst} - |X_{i,G}|)', \tag{9}$$

where $X_{i,G}$, $X_{i,G+1}$ denote the position vectors in the current iteration and the next iteration, respectively. $|X_{i,G+1}|$ is the absolute value of $X_{i,G}$, $X_{i,best}$ represents the best solution in the current iteration, and $X_{i,worst}$ denotes the worst solution in the current iteration.

In addition, the positioning algorithm is improved in the search for the optimal position. If the coordinate of the individual exceeds the range of the room, then the coordinate of this individual position is moved to the room boundary.

Step 5: The algorithm iteration termination criteria.

The algorithm is terminated iteratively when the maximum number of iterations is N , and the global optimal solution X_{best} is obtained. Otherwise, the algorithm continues to search for the best solution using steps 3 and 4.

4. Simulation results and analysis

4.1. The simulation model setup

Table 1. Main parameters of the indoor VLP system.

Parameter	Value
Transmitter power of the LED, P_t	2.2 W
Coordinates of the four LEDs	$[5,0,6]$, $[0,0,6]$, $[0,5,6]$, $[5,5,6]$
Effective area of the PD, A	1 cm^2
Half-power angle of the LED, $\phi_{1/2}$	60°
FOV of the PD, ψ_c	90°
Refractive index, n	1.5
Conversion efficiency of the PD, R_p	0.5 A/W
SNR of the positioning system, *SNR*	45dB
Population size, N_p	50
Variable dimension, D	3
Max iteration number, N	100

To verify the localization capability of the proposed algorithm, simulation experiments are performed in an indoor environment as shown in Figure 1, and the size of the room is 5 m × 5 m × 6 m. As signal generators, four LEDs are installed on the top of the room. Each LED transmits the encoding information based on CDMA modulation, which is subsequently received by the PD. The main parameters are set as displayed in Table 1. The simulations are performed with MATLAB on a computer (AMD Ryzen 5 @ 3 GHz, 16 GB of RAM, Windows 10).

4.2. Results and discussions

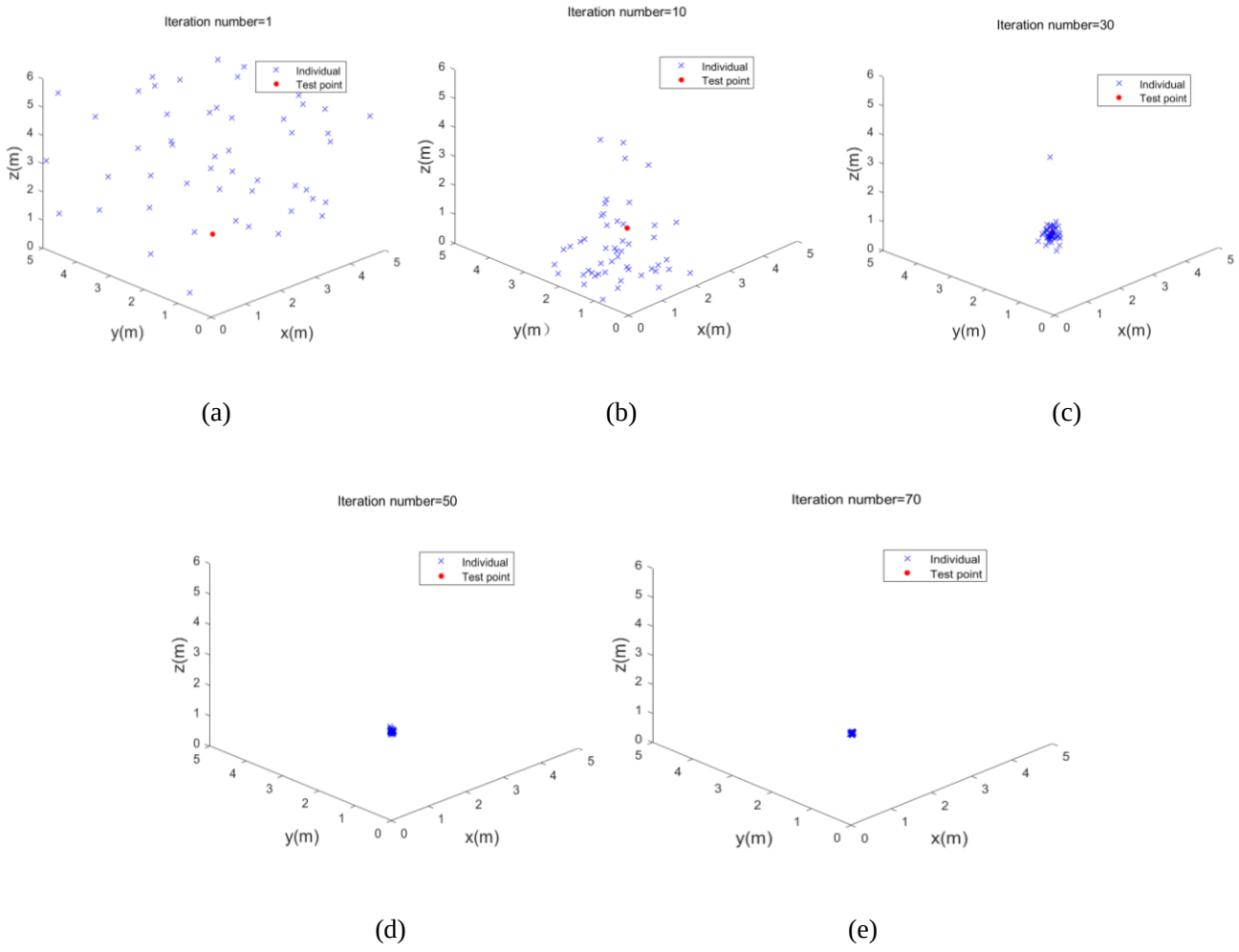

Figure 4. Iterative search process of the Jaya algorithm.

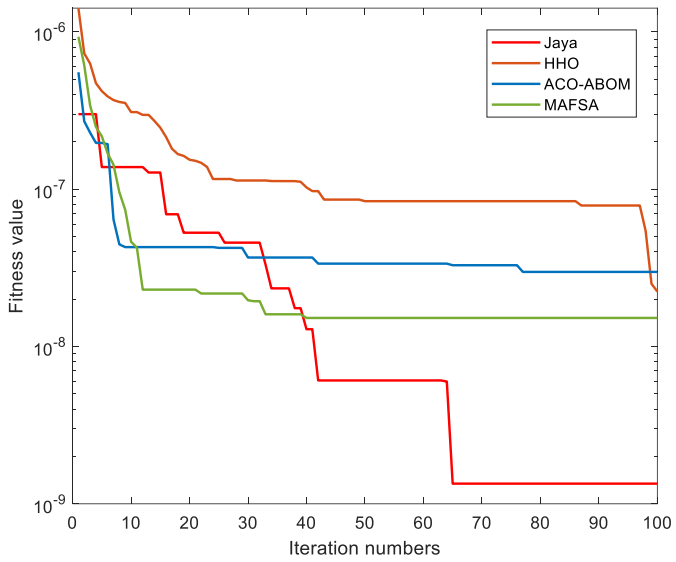

Figure 5. Convergence of the fitness values of the Jaya, HHO, ACO-ABOM and MAFSA algorithms.

The simulations are performed for a single point (1.5, 1.5, 1.5) (m) to validate the effectiveness of the Jaya algorithm. The convergence process of the algorithm is shown in Figures 4(a)–(e), where the blue cross represents the scattered individuals of the Jaya algorithm and the red dot represents the test point. In the initialization step of the algorithm, 50 individuals are randomly distributed in the space, many individuals moved toward the test point with increasing iteration number, and after 70 iterations all the scattered individuals concentrate at the test point. The final estimated position for this optimization is (1.4964, 1.5064, 1.5074) (m), the fitness function value is 1.3434×10^{-9}, and the estimation error of 3D positioning is 1.05 cm.

Next, Harris Hawks optimization (HHO) algorithm [40], ant colony algorithm with an ACO-ABOM [41] and modified artificial fish swam algorithm (MAFSA) [42] are simulated to validate the superior property of the Jaya algorithm. The simulation experiments are implemented in the same simulation environment for the above-mentioned algorithms. Figure 5 shows the convergence curves of the Jaya, HHO, ACO-ABOM and MAFSA algorithms. From Figure 5, the Jaya algorithm achieves a higher solution accuracy than the HHO, ACO-ABOM and MAFSA algorithms.

To demonstrate the capability of the proposed algorithm for multiple points, the test positions are placed at different heights (1.0, 2.0 and 3.0 m), while 361 test points are produced at each height. The cumulative distribution function (CDF) of the localization error is employed to represent the optimization performance of the algorithm.

With the Jaya optimization iterations, high-accuracy position estimation can be obtained for each test point. The intelligent algorithm search iterations are randomized, which can lead to large errors. To reduce the estimation error, for each test point, the algorithm is independently run 30 times and the best position is chosen from the run results. Figures 6(a)–(e) indicate the location of the test and estimation points at different heights. From Figures 6(a)–(c), the "×" symbol represents the test positions and the "△" symbol denotes the estimated positions. It can be seen that the estimated positions have a small estimation error with the test positions, which demonstrates the accuracy of visible light localization.

Figures 6(d),(e) show the histograms of the positioning errors and the CDF curves for all the test points, respectively. As shown in Figure 6(d), the average error of 3D positioning is 1.06 cm. In addition, it can be observed from Figure 6(e), if 95% is an acceptable coverage rate for location services, the 3D, horizontal, and vertical positioning errors of the Jaya are less than 2.308 cm, 1.806 cm and 1.895 cm, respectively.

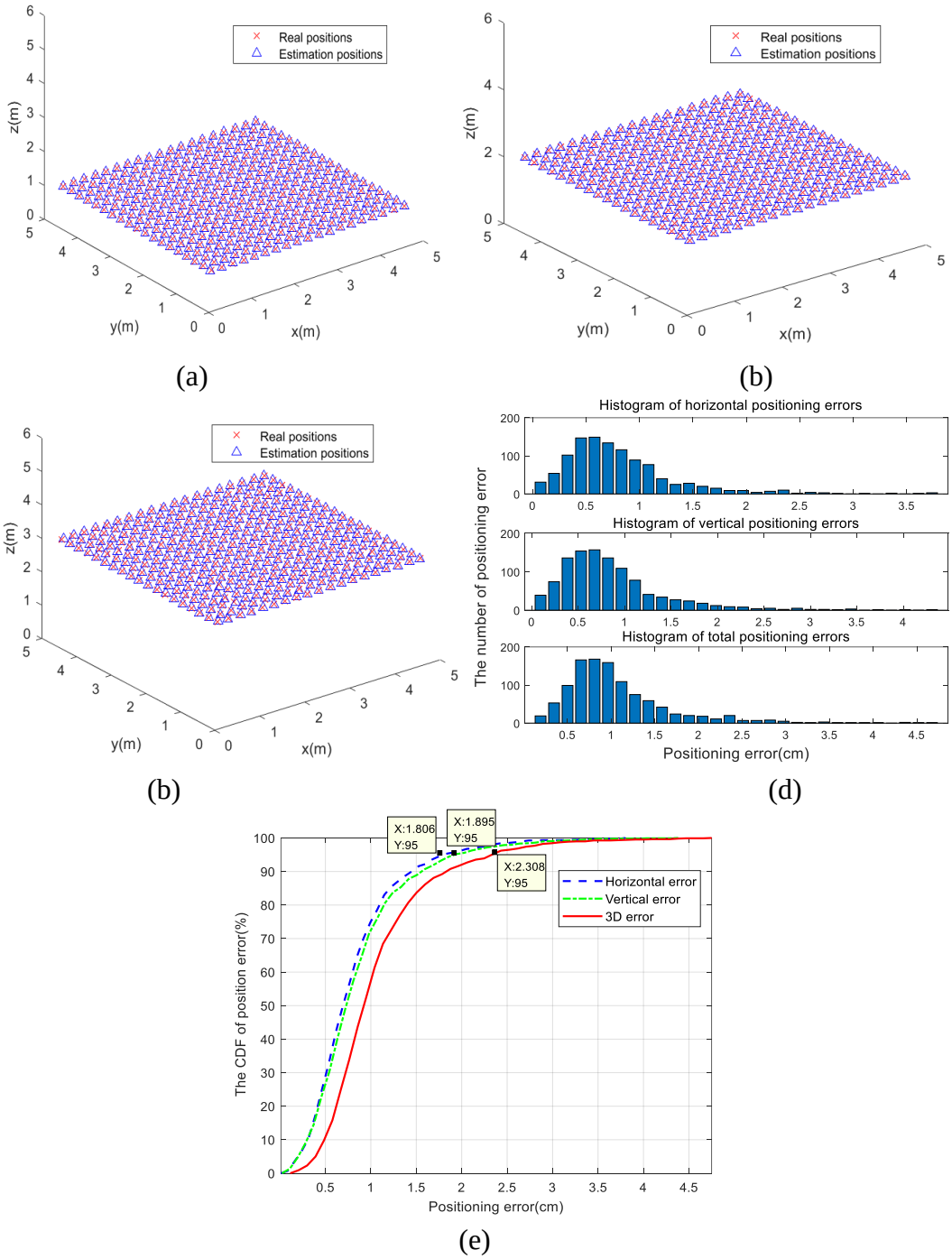

Figure 6. The test position and its estimated position. (a) Representation of test position and its estimated position (z = 1 m). (b) Representation of test position and its estimated position (z = 2 m). (c) Representation of test position and its estimated position (z = 3 m). (d) Histograms of the location errors. (e) CDF curves of the location error.

The HHO, ACO-ABOM and MAFSA algorithms are simulated with multiple points to further validate the efficiency of the Jaya algorithm. The positioning results of different algorithms are listed in Table 2. The histograms of positioning error and the CDF curves obtained with the Jaya, HHO, ACO-ABOM and MAFSA algorithms are shown in Figures 7 and 8, respectively. From Table 2, the average error of 3D positioning with the Jaya, HHO, ACO-ABOM, and MAFSA algorithms are 1.06 cm, 2.21 cm, 1.86 cm and 1.56 cm, respectively. The average localization times of the Jaya, HHO, ACO-ABOM, and MAFSA algorithms are 0.52 s, 1.08 s, 0.78 s and 0.92 s, respectively. From Figure 7, the positioning error of the Jaya is better than the HHO, ACO-ABOM and MAFSA algorithms. It can be observed from Figure 8 that, if 95% is an acceptable coverage rate for location services, the errors of 3D positioning using the Jaya, HHO, ACO-ABOM, and MAFSA algorithms are less than 2.308 cm, 5.321 cm, 3.405 cm and 2.918 cm, respectively. The simulation results indicate that the Jaya algorithm highly outperforms the HHO, ACO-ABOM and MAFSA algorithms.

Table 2. Positioning results of different algorithms.

Algorithm	Average positioning error	Maximum positioning error	Minimum positioning error	Average positioning time
Jaya	1.06 cm	4.75 cm	0.11 cm	0.52 s
HHO	2.21 cm	12.53 cm	0.22 cm	1.08 s
ACO-ABOM	1.86 cm	5.80 cm	0.13 cm	0.78 s
MAFSA	1.56 cm	5.50 cm	0.15 cm	0.92 s

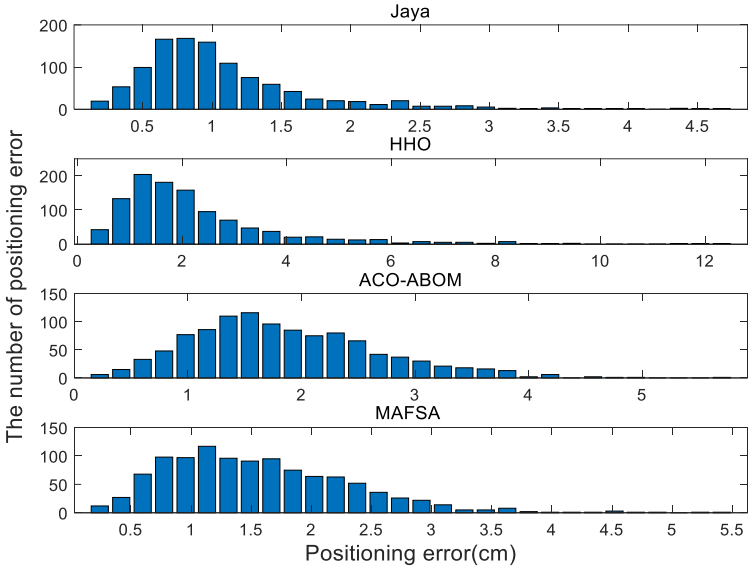

Figure 7. Histograms of the positioning errors of the Jaya, HHO, ACO-ABOM, and MAFSA algorithms.

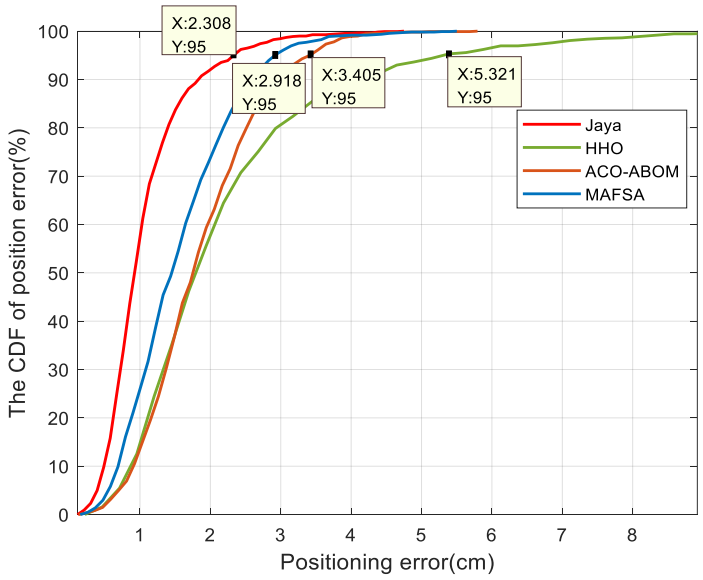

Figure 8. Cumulative distribution curves of the Jaya, HHO, ACO-ABOM, and MAFSA algorithms.

4.3. Extended result analysis

A simulation of trajectory tracking is performed to assess the effectiveness of the Jaya algorithm in motion scenes. In this simulation, it is assumed that the target object moves in a 3D room to generate a spiral path and 315 points are considered as test points on the path.

The location results of the Jaya algorithm in motion scenes are shown in Figures 9(a)–(e). In Figures 9(a)–(c), the blue line indicates the real movement path of the PD, and the red dots represent the estimated positions. The results of 3D, horizontal, and vertical positioning show that the estimated locations have a small estimation error with the true path. As shown in Figure 9(d), the average error of 3D location is 0.84 cm, the vertical location error is 0.68 cm, and the horizontal location error is 0.67 cm. Finally, it can be seen from Figure 9(e), if 95% is an acceptable coverage rate for location services, the 3D, vertical, and horizontal location errors of the Jaya algorithm are less than 1.463 cm, 1.338 cm and 1.315 cm, respectively.

The simulation of the HHO, ACO-ABOM and MAFSA algorithms are conducted in motion scenes. The positioning results of different algorithms are displayed in Table 3. The histograms of positioning error and the CDF curves are displayed in Figures 10 and 11, respectively. From Table 3, the average errors of 3D positioning with the Jaya, HHO, ACO-ABOM, and MAFSA algorithms are 0.84 cm, 1.28 cm, 1.33 cm and 1.21 cm, respectively. The average positioning times of the Jaya, HHO, ACO-ABOM, and MAFSA algorithms are 0.44 s, 0.95 s, 0.69 s and 0.85 s, respectively. From Figure 10, the positioning error of the Jaya algorithm is obviously superior to the HHO, ACO-ABOM, and MAFSA algorithms. As shown in Figure 11, if 95% coverage is considered acceptable for location services, the average errors of 3D positioning using the Jaya, HHO, ACO-ABOM, and MAFSA algorithms are less than 1.463 cm, 2.320 cm, 2.489 cm and 2.236 cm, respectively. As a result, the Jaya algorithm has a lower average localization error than the HHO, ACO-ABOM and MAFSA algorithms. The positioning time of the Jaya algorithm is less than those of the HHO, ACO-ABOM, and MAFSA algorithms. The simulation results also validate the Jaya algorithm's superiority performance in motion scenarios.

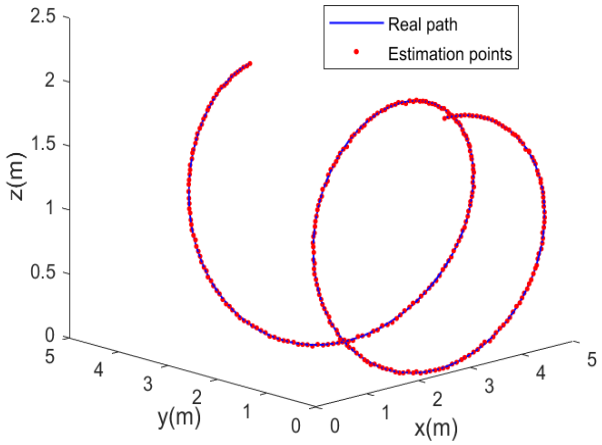

(a) The results of 3D location.

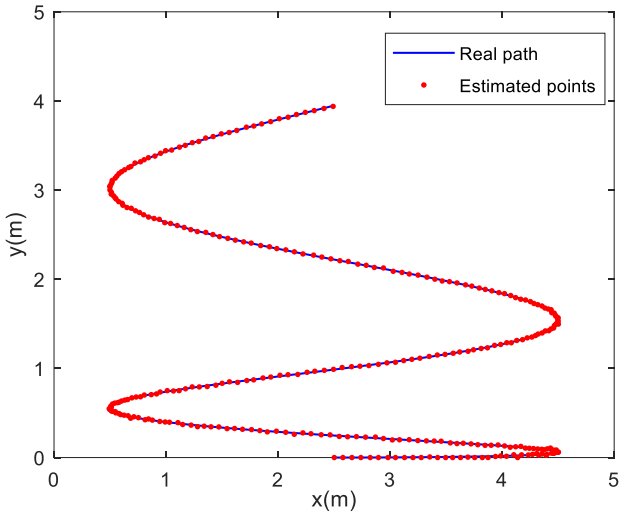

(b) The results of vertical location.

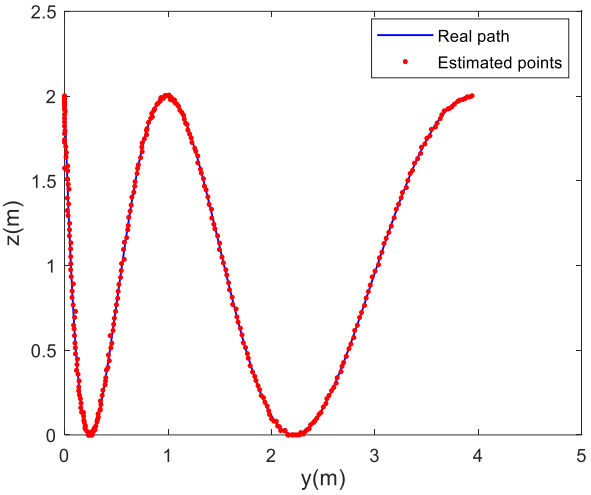

(c) The results of horizontal positioning.

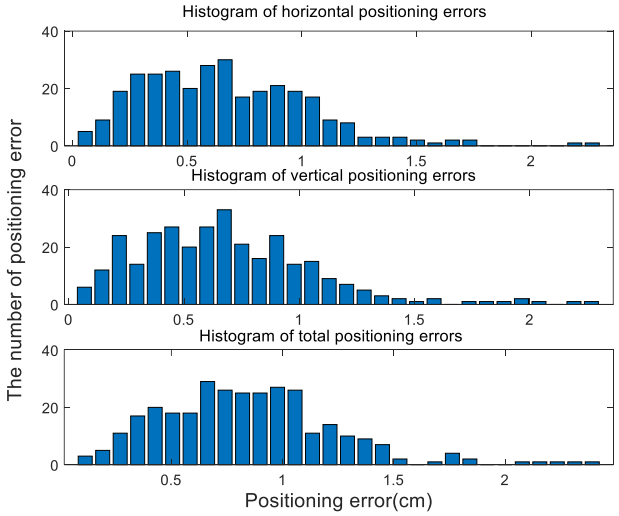

(d) Histograms of location error.

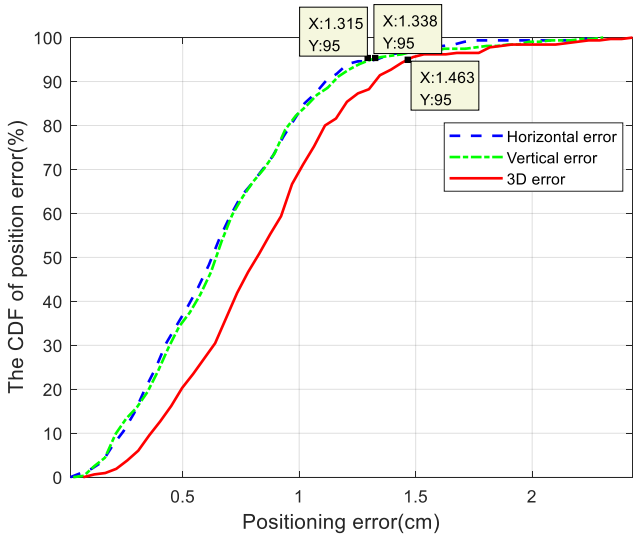

(e) CDF curves of location error.

Figure 9. Positioning results in motion scenes.

Table 3. Positioning results of different algorithms in motion scenes.

Algorithm	Average positioning error	Maximum positioning error	Minimum positioning error	Average positioning time
Jaya	0.84 cm	4.75 cm	0.01 cm	0.44 s
HHO	1.28 cm	3.42 cm	0.21 cm	0.95 s
ACO-ABOM	1.33 cm	3.32 cm	0.12 cm	0.69 s
MAFSA	1.21 cm	4.25 cm	0.18 cm	0.85 s

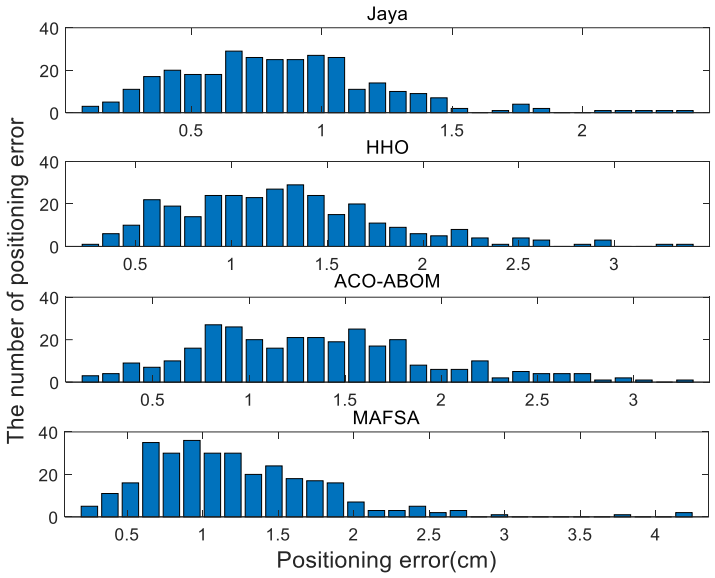

Figure 10. Histograms of the positioning errors of different algorithms in motion scenes.

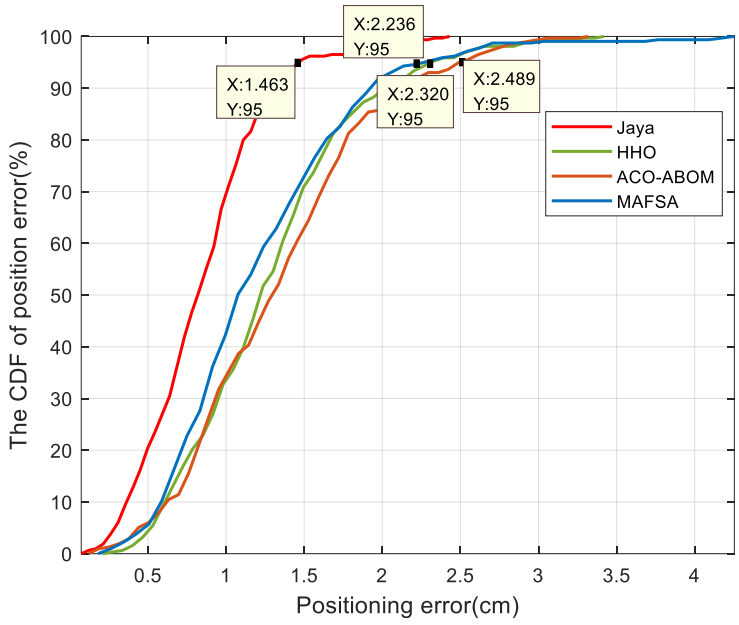

Figure 11. Cumulative distribution curves of different algorithms in motion scenes.

5. Conclusions

This study presented an indoor VLP system with the Jaya algorithm, which effectively improves positioning accuracy. The Jaya algorithm has a simple structure with only one stage, and the 3D positioning problem can be solved by the Jaya algorithm according to the positioning principle of RSS. The effectiveness of the algorithm is verified with a multipoint test in stationary scenes. The simulation results indicated that the Jaya algorithm has better localization accuracy and positioning time compared with the HHO, ACO-ABOM and MAFSA algorithms. Furthermore, simulation experiments are performed in motion scenes, and the Jaya algorithm also obtained good positioning accuracy. The proposed method efficiently improves the positioning accuracy of indoor VLP systems and has broad application prospects.

In future work, we will optimize the performance of the proposed algorithm and demonstrate the localization performance using a realistic VLP system with a robotic platform.

Acknowledgments

This research was funded by the National Natural Science Fund Projects of China (Grant No.61702375), the Anhui University Provincial Natural Science Research Project of China (Grant Nos. KJ2020A0636, KJ2021A1164, 2022AH051669 and 2022AH051683), the Natural Science Key Scientific Research Project of West Anhui University (Grant No.WXZR202103), and the Intelligent Networked Vehicle Key Technology Laboratory of Lu'an City.

Conflict of interest

All authors declare no conflicts of interest in this paper.

References

1. M. Yasir, S. W. Ho, B. N. Vellambi, Indoor positioning system using visible light and accelerometer, *J. Lightwave Technol.*, **32** (2014), 3306–3316. https://doi.org/10.1109/JLT.2014.2344772
2. W. Zhang, M. I. S. Chowdhury, M. Kavehrad, Asynchronous indoor positioning system based on visible light communications, *Opt. Eng.*, **53** (2014). https://doi.org/10.1117/1.OE.53.4.045105
3. H. Steendam, T. Q. Wang, J. Armstrong, Theoretical lower bound for indoor visible light positioning using received signal strength measurements and an aperture-based receiver, *J. Lightwave Technol.*, **35** (2017), 309–319. https://doi.org/10.1109/JLT.2016.2645603
4. K. Maaloul, B. Lejdel, E. Clementini, N. M. Abdelhamid, Bluetooth beacons based indoor positioning in a shopping malls using machine learning, *Bull. Electr.Eng. Inf.*, **12** (2023), 911–921. https://doi.org/10.11591/eei.v12i2.4200
5. C. Rizos, A. G. Dempster, B. H. Li, J. Salter, *Indoor Positioning Techniques Based on Wireless LAN*, (2007).
6. A. Poulose, D. S. Han, UWB indoor localization using deep learning LSTM networks, *Appl. Sci.*, **10** (2020), 6290. https://doi.org/10.3390/app10186290

7. E. Gonendik, S. Gezici, Fundamental limits on RSS based range estimation in visible light positioning systems, *IEEE Commun. Lett.*, **19** (2015), 2138–2141. https://doi.org/10.1109/LCOMM.2015.2493532
8. L. Huang, S. Wen, Z. Yan, H. Song, S. Su, W. Guan, Single LED positioning scheme based on angle sensors in robotics, *Appl. Opt.*, **60** (2021), 6275–6287. https://doi.org/10.1364/AO.425744
9. W. Guan, S. Wen, L. Liu, H. Zhang, High-precision indoor positioning algorithm based on visible light communication using complementary metal–oxide–semiconductor image sensor, *Opt. Eng.*, **58** (2019). https://doi.org/10.1117/1.OE.58.2.024101
10. W. Guan,Y. Wu, S. Wen, H. Chen, C. Yang,Y. Chen, et al., A novel three-dimensional indoor positioning algorithm design based on visible light communication, *Opt. Commun.*, **392** (2017), 282–293. https://doi.org/10.1016/j.optcom.2017.02.015
11. W. Guan, S. Chen, S. Wen, Z. Tan, H. Song, W. Hou, High-accuracy robot indoor localization scheme based on robot operating system using visible light positioning, *IEEE Photonics J.*, **12** (2020), 1–16. https://doi.org/10.1109/JPHOT.2020.2981485
12. J. Chen, D. Zeng, C. Yang, W. Guan, High accuracy, 6-DoF simultaneous localization and calibration using visible light positioning, *J. Lightwave Technol.*, **40** (2022), 7039–7047. https://doi.org/10.1109/JLT.2022.3198649
13. M. F. Keskin, S. Gezici, O. Arikan, Direct and two-step positioning in visible light systems, *IEEE Trans. Commun.*, **66** (2018), 239–254. https://doi.org/10.1109/TCOMM.2017.2757936
14. H. Liu, H. Darabi, P. Banerjee, J. Liu, Survey of wireless indoor positioning techniques and systems, *IEEE Trans. Syst., Man Cybern., Part C (Appl. Rev.)*, **37** (2007), 1067–1080. https://doi.org/10.1109/TSMCC.2007.905750
15. E. Kazikli, S. Gezici, Hybrid TDOA/RSS based localization for visible light systems, *Digit. Signal Process.*, **86** (2019), 19–28. https://doi.org/10.1016/j.dsp.2018.12.001
16. N. Chaudhary, L. N. Alves, Z. Ghassemlooy, Impact of transmitter positioning and orientation uncertainty on RSS-based visible light positioning accuracy, *Sensors (Basel)*, **21** (2021), 3044. https://doi.org/10.3390/s21093044
17. J. Lui, A. M. Vegni, L. Colace, A. Neri, C. Menon, Preliminary design and characterization of a low-cost and low-power visible light positioning system, *Appl. Opt.*, **58** (2019), 7181–7188. https://doi.org/10.1364/AO.58.007181
18. Y. Sun, X. Wang, Y. Chen, Z. Liu, A modified whale optimization algorithm for large-scale global optimization problems, *Expert Syst. Appl.*, **114** (2018), 563–577. https://doi.org/10.1016/j.eswa.2018.08.027
19. H. Haklı, H. Uğuz, A novel particle swarm optimization algorithm with Levy flight, *Appl. Soft Comput.*, **23** (2014), 333–345. https://doi.org/10.1016/j.asoc.2014.06.034
20. S. M. Bozorgi, S. Yazdani, IWOA: An improved whale optimization algorithm for optimization problems, *J. Comput. Des. Eng.*, **6** (2019), 243–259. https://doi.org/10.1016/j.jcde.2019.02.002
21. L. Wang, F. Li, J. Xing, A hybrid artificial bee colony algorithm and pattern search method for inversion of particle size distribution from spectral extinction data, *J. Mod. Opt.*, **64** (2017), 2051–2065. https://doi.org/10.1080/09500340.2017.1337250
22. W. Li, K. Zhong, Application of improved particle swarm optimization algorithm in solving camera extrinsic parameters, *J. Mod. Opt.*, **66** (2019), 1827–1835. https://doi.org/10.1080/09500340.2019.1682203

23. E. H. Houssein, M. E. Hosney, M. Elhoseny, D. Oliva,W. M. Mohamed, M. Hassaballah, Hybrid Harris Hawks optimization with cuckoo search for drug design and discovery in chemoinformatics, *Sci. Rep.*, **10** (2020), 14439. https://doi.org/10.1038/s41598-020-71502-z
24. H. Chen, W. Guan, S. Li, Y. Wu, Indoor high precision three-dimensional positioning system based on visible light communication using modified genetic algorithm, *Opt. Commun.*, **413** (2018), 103–120. https://doi.org/10.1016/j.optcom.2017.12.045
25. Y. Chen, H. Zheng, H. Liu, Z. Han, Z. Ren, Indoor high precision three-dimensional positioning system based on visible light communication using improved hybrid bat algorithm, *IEEE Photonics J.*, **12** (2020). https://doi.org/10.1109/JPHOT.2020.3017670
26. L. Huang, P. Wang, Z. Liu, X. Nan, L. Jiao, L. Guo, Indoor three-dimensional high-precision positioning system with bat algorithm based on visible light communication, *Appl. Opt.*, **58** (2019), 2226–2234. https://doi.org/10.1364/AO.58.002226
27. Y. Chen, Z. Ren, Z. Han, H. Liu, Q. Shen, Z. Wu, LED based high accuracy indoor visible light positioning algorithm, *Optik*, **243** (2021), 166853. https://doi.org/10.1016/j.ijleo.2021.166853
28. Y. Wu, X. Liu, W. Guan, B. Chen, X. Chen, C. Xie, High-speed 3D indoor localization system based on visible light communication using differential evolution algorithm, *Opt. Commun.*, **424** (2018), 177–189. https://doi.org/10.1016/j.optcom.2018.04.062
29. W. Guan, Y. Wu, C. Xie, H. Chen, Y. Cai, Y. Chen, High-precision approach to localization scheme of visible light communication based on artificial neural networks and modified genetic algorithms, *Opt. Eng.*, **56** (2017), 106103. https://doi.org/10.1117/1.OE.56.10.106103
30. A. A. Mahmoud, Z. U. Ahmad, O. C. L. Haas, S. Rajbhandari, Precision indoor three-dimensional visible light positioning using receiver diversity and multi-layer perceptron neural network, *IET Optoelectron.*, **14** (2020), 440–446. https://doi.org/10.1049/iet-opt.2020.0046
31. R. V. Rao, A. Saroj, An elitism-based self-adaptive multi-population Jaya algorithm and its applications, *Soft Comput.*, **23** (2018), 4383–4406. https://doi.org/10.1007/s00500-018-3095-z
32. M. A. Dawood, S. S. Saleh, E. S. A. El-Badawy, M. H. Aly, A comparative analysis of localization algorithms for visible light communication, *Opt. Quantum Electron.*, **53** (2021). https://doi.org/10.1007/s11082-021-02751-z
33. A. Poulose, An optisystem simulation for indoor visible light communication system, in *National Conference on Emerging Technologies (NCET)*, (2017).
34. A. Poulose, Simulation of an indoor visible light communication system using optisystem, *Signals*, **3** (2022), 765–793. https://doi.org/10.3390/signals3040046
35. T. Komine, M. Nakagawa, Fundamental analysis for visible-light communication system using LED lights, *IEEE Trans. Consumer Electron.*, **50** (2004), 100–107. https://doi.org/10.1109/TCE.2004.1277847
36. H. Lu, B. Ba, W. J. Cui, A novel fusion visible light location algorithm based on rssi and imaging of LEDs, *Proc. Comput. Sci.*, **107** (2017), 848–854. https://doi.org/10.1016/j.procs.2017.03.180
37. R. Venkata Rao, Jaya: A simple and new optimization algorithm for solving constrained and unconstrained optimization problems, *Int. J. Ind. Eng. Comput.*, (2016), 19–34. https://doi.org/10.5267/j.ijiec.2015.8.004
38. X. Z. Jian, Z. Y. Weng, A logistic chaotic JAYA algorithm for parameters identification of photovoltaic cell and module models, *Optik*, **203** (2020). https://doi.org/10.1016/j.ijleo.2019.164041

39. C. C. Jia, Y. Ting, C. J. Wang, M. L. Sun, High-Accuracy 3D indoor visible light positioning method based on the improved adaptive cuckoo search algorithm, *Arabian J. Sci. Eng.*, **47** (2022), 2479–2498. https://doi.org/10.1007/s13369-021-06144-y
40. A. A. Heidari, S. Mirjalili, H. Faris, I. Aljarah, M. Mafarja, H. Chen, Harris Hawks optimization: Algorithm and applications, *Future Gener. Comput. Syst.*, **97** (2019), 849–872. https://doi.org/10.1016/j.future.2019.02.028
41. Y. Chen, J. Li,S. Wen, W. Guan, J. Jiang, B. Chen, Performance comparison and analysis on different optimization models for high-precision three-dimensional visible light positioning, *Opt. Eng.*, **57** (2018). https://doi.org/10.1117/1.OE.57.12.125101
42. M. Huang, B. Chen, J. Jiang, W. Guan, X. Cai, S. Wen, High-precision indoor three-dimensional positioning system based on visible light communication using modified artificial fish swarm algorithm, *Opt. Eng.*, **57** (2018), 106102. https://doi.org/10.1117/1.OE.57.10.106102

AIMS Press